

Approximations to linear wave scattering by  
topography using an integral equation  
approach

September 16, 2005

## **Abstract**

This dissertation considers approximations to the scattering of a train of small-amplitude harmonic surface waves on water by topography, using the mild-slope equation and the modified mild-slope equation. The associated boundary value problem is converted into two real-valued integral equations, the solutions of which are approximated by variational techniques. The reproduction of existing results over different shaped taluds are considered and show that this integral equation method is an equally effective solution technique as existing approximate numerical differential equation techniques. Finally, a ripple bed example is considered and it is reaffirmed that the modified mild-slope equation is capable of producing more accurate approximations over a wider range of topographies than the mild-slope equation.

This dissertation is based on the work of Chamberlain (1993).

## Acknowledgements

I wish to thank Doctors Peter Chamberlain and Nick Biggs for their support during this dissertation. Their inexhaustible supply of help, advice and most importantly patience has been invaluable in the completion of this dissertation. In addition I wish to thank the EPSRC for their grant, without which I would not have been able to study this course, and my classmates who have provided many light-hearted moments this year.

Outside of academic circles, I wish to thank my mum Linda, who has put up with phone call after phone call of ceaseless moaning and defeatism for weeks. Likewise, thanks must go to my wonderful fiancée Miss Rachel Porter, who has provided copious amounts of support, hugs and (most importantly) coffee.

Finally, I wish to dedicate this dissertation to my father Philip Chidlow. He never stopped believing in my ability to get things done even when I didn't believe in myself and more importantly, he always used to make me laugh. I miss you dad.

## **Declaration**

I confirm that this is my own work, and the use of all material from other sources has been properly and fully acknowledged.

STEWART JOHN CHIDLOW

# Contents

<b>1</b>	<b>Introduction</b>	<b>6</b>
<b>2</b>	<b>Integral equations</b>	<b>8</b>
2.1	The classification of integral equations . . . . .	8
2.2	Integral operators . . . . .	10
2.3	Galerkin's method . . . . .	10
2.4	The Petrov-Galerkin method . . . . .	12
<b>3</b>	<b>The modified mild-slope and mild-slope equations</b>	<b>13</b>
3.1	The wave scattering problem . . . . .	13
3.2	Derivation of the modified mild-slope equation . . . . .	14
3.3	The mild-slope equation . . . . .	16
<b>4</b>	<b>Formulation of the wave scattering problem</b>	<b>18</b>
4.1	Class of depth profiles . . . . .	18
4.2	Boundary conditions . . . . .	20
4.3	Conversion to an integral equation . . . . .	23
<b>5</b>	<b>Methods of solution</b>	<b>29</b>
5.1	Inner product approximations . . . . .	32

5.2	Choice of basis functions . . . . .	34
<b>6</b>	<b>Numerical results</b>	<b>36</b>
6.1	Booij's test problem . . . . .	36
6.1.1	Dimension of the trial spaces . . . . .	39
6.1.2	Accuracy of the Neumann series . . . . .	43
6.1.3	Booij's test problem using the MSE and MMSE subject to two different sets of boundary conditions . . . . .	44
6.2	The effects of different types of talud on the reflection coefficients	47
6.3	Wave scattering over ripple beds . . . . .	49
<b>7</b>	<b>Conclusions</b>	<b>54</b>

# List of Figures

6.1	Reproduction of Booij's graph using our solution procedure plotted against the full linear solution. . . . .	39
6.2	Number of basis functions needed to make the error $< 10^{-2}$ . . . . .	40
6.3	Number of basis functions needed to make the error $< 10^{-4}$ . . . . .	41
6.4	No. of basis functions needed to make the error $< 10^{-6}$ . . . . .	42
6.5	A comparison between the Petrov-Galerkin approximation and the Neumann series approximation applied to Booij's test problem. . . . .	44
6.6	Comparison of the MSE and MMSE subject to continuous boundary conditions applied to Booij's test problem. . . . .	46
6.7	Comparison of the MSE and MMSE subject to discontinuous boundary conditions applied to Booij's test problem. . . . .	47
6.8	The effect of different bed shapes on $ R_1 $ . . . . .	49
6.9	Comparison of computed reflection coefficients for a ripple bed problem with $n = 4$ and $\delta = 0.32$ . . . . .	52
6.10	Comparison of computed reflection coefficients for a ripple bed problem with $n = 10$ and $\delta = 0.16$ . . . . .	52

# Chapter 1

## Introduction

A long-standing problem in water wave theory is the determination of the influence of bed topography on an incident wave train. This is of considerable importance in coastal engineering where the shape of the seabed, and in some instances man-made obstacles, can dramatically effect wave behaviour (e.g. predicting wave heights in harbours). These problems involve a combination of the scattering, diffraction and refraction of waves and are difficult problems to solve.

This dissertation is concerned with the effect on waves of bed topography. The situation considered is where two regions of constant depth (not necessarily equal) are joined by a hump occupying a finite region in the seabed. The linearised equations for modelling such a flow are widely known but unfortunately there are rarely any existing analytic solutions except in very simple cases where vertical and/or horizontal boundaries are used. As a result of this, the mild slope approximation is used in order to generate the problem and then the resulting boundary value problem is transformed into

an integral equation to be solved.

An alternate approximation to the mild-slope equation has also been derived in recent years. This approximation is widely believed to be better than the mild-slope equation as experimental results have shown a higher level of accuracy in the wave predictions using the modified-mild slope equation over a wider range of bed topographies. This dissertation includes comparisons between both equations and considers the reproduction of other people's results in order to illustrate any differences that occur.

Although the method of integral equations has been applied to the mild-slope equation in order to solve the wave-scattering problem, it is the author's belief that no-one else has attempted to use the method of integral equations to solve the modified-mild slope equation.

# Chapter 2

## Integral equations

Integral equations occur widely in many areas of applied mathematics. An integral equation is very similar to a differential equation except that it involves an integral of an unknown function rather than its derivatives. Differential equations and integral equations are often interchangeable, in the sense that a boundary value problem can be formulated as a differential equation or an equivalent integral equation. In the following chapters we replace an ordinary differential equation by an equivalent integral equation in order to take advantage of the powerful solution techniques available for such equations.

### 2.1 The classification of integral equations

Integral equations are classified according to four different criteria:

- the kind of the integral equation;
- the interval of integration;
- whether the equation is regular or singular;

- whether the equation is homogeneous or inhomogeneous.

The ‘kind’ of an integral equation refers to where the unknown function appears in the equation. If the unknown function only appears under the integral sign then the equation is said to be *first-kind*, whereas if it appears outside the integral sign as well then it is said to be *second kind*.

The interval of integration determines whether the integral equation is a *Volterra* equation or a *Fredholm* equation. If the interval of integration is definite then the equation is said to be a Fredholm equation. If however the interval of integration is indefinite then the equation is said to be a Volterra equation.

The equation is said to be *singular* if the interval of integration is indefinite or if the integrand is unbounded at any one or more points in the interval specified. Correspondingly if the integral is definite and the integrand is bounded and well defined at every point in the interval specified, then the equation is said to be *regular*.

Finally, an integral equation is said to be *homogeneous* if  $f$  is equal to zero or *inhomogeneous* if  $f$  is non-zero. The former case typically corresponds to an eigenvalue problem.

## 2.2 Integral operators

An example of a second kind, Fredholm integral equation is

$$\chi(x) = f(x) + \lambda \int_a^b k(x, t)\chi(t)dt,$$

where  $\lambda$  is a constant,  $f(x)$  is a *forcing term* and the function  $k(x, t)$  is called the kernel of the function and can be real or complex-valued. This again is to be solved for the unknown function  $\chi$ . We can introduce the operator  $K$  such that

$$(K\chi)(x) = \int_a^b k(x, t)\chi(t)dt.$$

This allows us to rewrite the integral equation as an operator equation

$$\chi = f + K\chi.$$

on the infinite dimensional Hilbert space  $H(a, b)$  (typically  $L_2(a, b)$ ). In addition to the obvious benefits of working within a Hilbert space, this approach proves very useful from the notational point of view.

## 2.3 Galerkin's method

Galerkin's method is used to provide approximations to the solutions of inhomogeneous integral equations.

Suppose we are trying to find an approximation to the integral equation

$$A\chi = f,$$

where  $A$  is defined as

$$A = (I - \lambda K).$$

We seek to approximate the solution of the equation in the  $N$  dimensional subspace  $E_N$  of  $H$  spanned by the test functions  $\psi_1, \dots, \psi_N$ . We write

$$\chi \simeq p = \sum_{n=1}^N a_n \psi_n, \quad (2.1)$$

where the  $a_n$  are coefficients yet to be determined.

In practice it is highly unlikely that this approximation will satisfy the integral equation exactly so we instead ask that the components of the equation which lie in  $E_N$  are satisfied. This means that we require

$$(Ap - f, \psi_m) = 0 \quad (m = 1, \dots, N), \quad (2.2)$$

where  $p$  is as before. If we now substitute the expression (2.1) into equation (2.2), we obtain

$$\left( \sum_{n=1}^N a_n A\psi_n - f, \psi_m \right) = 0, \quad (m = 1, \dots, N) \quad (2.3)$$

which is equivalent to

$$\sum_{n=1}^N (a_n A \psi_n, \psi_m) = (f, \psi_m), \quad (m = 1, \dots, N). \quad (2.4)$$

This gives an  $N \times N$  matrix system which is solved for the coefficients  $a_n$ . This solution technique is called Galerkin's method.

## 2.4 The Petrov-Galerkin method

The Petrov-Galerkin method is a very similar solution technique to Galerkin's method. The difference between the two methods is very subtle.

The expression we had previously in equation (2.2) tells us to make  $Ap - f$  orthogonal to the basis functions  $\psi_n$  in an attempt to satisfy a weak form of the integral equation. However, we can instead choose to make  $Ap - f$  orthogonal to another set of functions  $\xi_n$ ,  $n = 1, \dots, N$  where the functions  $\xi_n$  are not the basis functions for  $p$  but are an alternate set of functions. This is the Petrov-Galerkin method.

# Chapter 3

## The modified mild-slope and mild-slope equations

### 3.1 The wave scattering problem

Let  $x$  and  $y$  be orthogonal horizontal coordinates and  $z$  be a vertical coordinate measured positive upwards with  $z = 0$  located at the undisturbed free surface and  $z = -h$  is the depth of the seabed. In this dissertation, the only fluids considered are assumed homogeneous, incompressible, in irrotational motion and inviscid. This implies that a harmonic velocity potential  $\Phi$  exists. We also assume that the surface disturbances are small enough for linearised theory to apply and that the motion is periodic in time with a given angular frequency  $\sigma$ . Assumption of periodic time dependence allow us to write

$$\Phi(x, y, z, t) = \Re(\phi(x, y, z)e^{-i\sigma t}).$$

The standard three-dimensional equations for fluid flow involve the use of Laplace's equation in three dimensions in order to solve the problem. However the modified mild-slope equation seeks to reduce the dimension of the problem by approximating the dependence of  $\phi$  on  $z$ .

### 3.2 Derivation of the modified mild-slope equation

It was stated in the previous section that the fluid we are considering is deemed incompressible and irrotational. This means that a velocity potential exists and satisfies Laplace's equation in three space dimensions. As we are only attempting to approximate the solution, we can seek a weak solution  $\xi \simeq \phi$  of Laplace's equation in the sense that  $\nabla^2 \xi$  is orthogonal to a given function  $w$ . Hence

$$\int \int_D \left( \int_{-h}^0 w \nabla^2 \xi dz \right) dx dy = 0.$$

The full detail of this derivation is included in Chamberlain and Porter (1995), but if we were to seek an approximation of this form, eventually we would obtain the approximation

$$\phi(x, y, z) \simeq \cosh(k(z + h)) \operatorname{sech}(kh) \phi_0(x, y)$$

where the function  $h(x, y)$  is the still water depth at the location  $(x, y)$  and the function  $\phi_0(x, y)$  is an approximation to the velocity potential at the linearised free surface. This approximation for  $\phi_0(x, y, z)$  in turn leads to the equation

$$\nabla \cdot (u \nabla \phi_0) + (k^2 u + u_1 \nabla^2 h + u_2 (\nabla h)^2) \phi_0 = 0, \quad (3.1)$$

where  $\nabla = (\frac{\partial}{\partial x}, \frac{\partial}{\partial y})$ , the function  $u$  is given by

$$u = \frac{\tanh(kh)}{2k} \left( 1 + \frac{2kh}{\sinh(2kh)} \right),$$

and the local wave number  $k = k(x, y)$  is the positive real root of

$$\frac{\sigma^2}{g} = k \tanh(kh).$$

The other functions  $u_1 = u_1(x, y)$  and  $u_2 = u_2(x, y)$  are defined as

$$u_1(x, y) = \frac{\operatorname{sech}^2(kh)}{4(K + \sinh(K))} (\sinh(K) - K \cosh(K))$$

and

$$u_2(x, y) = \frac{k \operatorname{sech}^2(kh)}{12(K + \sinh(K))^3} (K^4 + 4K^3 \sinh(K) - 9 \sinh(K) \sinh(2K) + 3K(K + 2 \sinh(K))(\cosh^2(K) - 2 \cosh(K) + 3)).$$

The abbreviation  $K = 2kh$  has been used above.

Equation (3.1) is known as the modified mild-slope equation.

### 3.3 The mild-slope equation

The mild-slope equation is an alternate approximation to the modified mild-slope equation. It can be easily obtained from (3.1) above by making the assumption that the second derivative of  $h$  and the square of its first derivative are negligibly small. This process results with

$$\nabla \cdot (u \nabla \phi_0) + k^2 u = 0 \tag{3.2}$$

which is the mild-slope equation.

The mild slope equation was the initial approximation used and was derived by Berkhoff (1973,1976). The paper that my dissertation has been based upon was written at a time when the mild-slope equation was a standard approximation to the function  $\phi(x, y, z)$  in the expression for the velocity potential  $\Phi(x, y, z, t)$ . However since this paper has been published, the modified mild-slope equation has been derived. This was initially derived because many authors had commented that the mild-slope equation was failing to produce adequate approximations for certain types of topography such as ripple beds (where a finite interval of varying depth consists

of small-amplitude sinusoidal ripples). This lack of accuracy led to many authors having to model ripple bed problems by alternate means. In 1995, Chamberlain and Porter developed the modified mild-slope equation as an alternate approximation technique. It has been found that this approximation can more accurately predict behaviour over a wider range of topographies.

The methods of solution discussed in the ensuing chapters are equally applicable to the modified mild-slope equation and the mild slope equation, the only difference being the inclusion of the extra two terms in the initial equation.

# Chapter 4

## Formulation of the wave scattering problem

The very basic problem has been set up in the previous chapter. We still make the same assumptions about the fluid and now begin to discuss the full formulation of the resulting problem. We consider the application of the mild-slope approximation to the problem so for the time being we are also making the additional assumptions about the derivatives of  $h$  laid out in the previous chapter.

### 4.1 Class of depth profiles

The class of depth profiles we consider are such that  $h$  is  $y$ -independent and varying in some finite interval of  $x$ . Outside this interval we assume that  $h$  is constant. Hence

$$h(x) = \begin{cases} h_0 & \forall x \leq 0 \\ h_1 & \forall x \geq l \end{cases}$$

where  $h_0$  and  $h_1$  are constant for a given problem and may or may not be equal. We further assume that  $h(x)$  is continuous. The final assumption we make is that the wave motion is such that the crests are parallel to the  $y$ -axis which implies that  $\phi_0 = \phi_0(x)$ . As we have now moved from two space dimensions to one space dimension, equation (3.2) becomes

$$\frac{d}{dx} \left( u \frac{d\phi_0}{dx} \right) + k^2 u \phi_0 = 0 \quad (4.1)$$

where now  $u$  and  $k$  only depend on  $x$ .

If we define a new function  $\zeta$  by

$$\zeta(x) = \phi_0(x) \sqrt{\frac{u(x)}{u(0)}}$$

then (4.1) is reduced to its canonical form

$$\zeta'' + k_0^2 \zeta = \rho \zeta \quad (4.2)$$

where

$$\rho(x) = \frac{u''(x)}{2u(x)} - \left( \frac{u'(x)}{2u(x)} \right)^2 + k_0^2 - k^2,$$

and  $k_0$  is the wavenumber corresponding to  $h_0$ . The primes here denote differentiation with respect to  $x$ .

We have written the equation in this format so that the coefficient of  $\zeta$  is a constant rather than a function of  $x$ . The reason for this will become apparent when we transform to an integral equation.

## 4.2 Boundary conditions

We now need to assign the incident waves in order to uniquely define the problem. For most of the project we consider the case of a hump in a finite region joining two regions of constant but different depths (a talud). This tells us that  $h_0 \neq h_1$  and hence  $k_0 \neq k_1$  ( $k_1$  is the wavenumber corresponding to  $h_1$ ).

We assume that there are two plane waves incident from  $x = \pm\infty$  with known complex amplitudes  $A^\pm$ . This results in two outgoing waves with unknown complex amplitudes  $B^\pm$ . Formally, we have

$$\phi_0(x) = \begin{cases} A^- e^{ik_0 x} + B^- e^{-ik_0 x} & \forall x \leq 0, \\ A^+ e^{-ik_1 x} + B^+ e^{ik_1 x} & \forall x \geq l, \end{cases}$$

and using our definition for  $\zeta$ , we have as a consequence

$$\zeta(x) = \begin{cases} A^- e^{ik_0 x} + B^- e^{-ik_0 x} & \forall x \leq 0, \\ (A^+ e^{-ik_1 x} + B^+ e^{ik_1 x}) \sqrt{\frac{u(l)}{u(0)}} & \forall x \geq l. \end{cases} \quad (4.3)$$

We now consider a restricted version of (4.2), namely

$$\zeta'' + k_0^2 \zeta = \rho \zeta, \quad 0 < x < l, \quad (4.4)$$

and use (4.3) to derive boundary conditions. In order to satisfy (4.1), we know that  $\phi_0$  and  $\phi_0'$  must be continuous. Hence we have that

$$\phi_0'(0-) = \phi_0'(0+)$$

and

$$\phi_0'(l-) = \phi_0'(l+).$$

If we differentiate (4.3) and implement the two equations above, we obtain the jump conditions

$$\zeta'(0-) = \zeta'(0+) - \frac{u'(0+)\zeta(0)}{2u(0)},$$

and

$$\zeta'(l+) = \zeta'(l-) - \frac{u'(l-)\zeta(l)}{2u(l)}.$$

This pair of equations tells us that although  $\zeta$  is continuous at  $x = 0$  and  $x = l$ , its first derivative is not continuous at these locations. Further substitution for  $\zeta(0)$  and  $\zeta(l)$  from (4.3) in turn leads to the boundary conditions

$$\zeta'(0) + \left( ik_0 - \frac{u'(0)}{2u(0)} \right) \zeta(0) = 2A^- ik_0 \quad (4.5)$$

and

$$\zeta'(l) - \left( ik_1 + \frac{u'(l)}{2u(l)} \right) \zeta(l) = -2A^+ ik_1 e^{-ik_1 l} \sqrt{\frac{u(l)}{u(0)}}. \quad (4.6)$$

The boundary value problem for  $\zeta$  consisting of (4.4), (4.5) and (4.6) is now uniquely defined and well-posed in  $(0, l)$ . In practice it is not necessary to have both  $A^-$  and  $A^+$  non-zero since the linearity of the problem allows us to superpose two solutions corresponding to single incident waves. In each case we can set the amplitude of the non-zero incident wave, without loss of generality, equal to one. In these cases, the two outgoing waves are known as the reflection and transmission coefficients. These coefficients are denoted by  $R$  and  $T$  with subscripts to distinguish between waves incident from the left or the right. This notation is summarised as follows

- if  $A^+ = 0$  then  $R_1 = \frac{B^-}{A^-}$  and  $T_1 = \frac{B^+}{A^-}$ ;

- if  $A^- = 0$  then  $R_2 = \frac{B^+}{A^+}$  and  $T_2 = \frac{B^-}{A^+}$ .

We can now use (4.3) to express the reflection and transmission coefficients in terms of  $\zeta$ . Thus

$$R_1 = \frac{\zeta(0)}{A^-} - 1, \quad T_1 = \left( \frac{\zeta(l)e^{-ik_1l}}{A^-} \right) \sqrt{\frac{u(0)}{u(l)}}; \quad (4.7)$$

$$R_2 = \left( \frac{\zeta(l)e^{-ik_1l}}{A^+} \right) \sqrt{\frac{u(0)}{u(l)}} - e^{-2ik_1l}, \quad T_2 = \frac{\zeta(0)}{A^+}. \quad (4.8)$$

These expressions illustrate that the solution for  $\zeta(x)$  in the interval  $(0, l)$  is not needed to determine the reflection and transmission coefficients; only the solution at the end-points is required.

### 4.3 Conversion to an integral equation

We now convert the boundary value problem into an integral equation. The conversion of a boundary value problem of the type defined by (4.4), (4.5) and (4.6) is fairly straightforward but some care is needed to avoid undue complexity.

Firstly we write  $\zeta = \zeta_0 + \hat{\zeta}$ . We choose  $\zeta_0$  to satisfy the boundary conditions (4.5) and (4.6) and the homogeneous equation

$$\zeta_0'' + k_0^2 \zeta_0 = 0.$$

As a result of this, we must choose  $\hat{\zeta}$  to satisfy the inhomogeneous equation subject to the homogeneous forms of (4.5) and (4.6). Hence

$$\hat{\zeta}'' + k_0^2 \hat{\zeta} = \rho \zeta.$$

These conditions would result in the integral equation having a complicated kernel. However, if we rewrite the boundary conditions as

$$\zeta'(0) + ik_0 \zeta(0) = 2ik_0(c_1 + c_2 \zeta(0) + c_3 \zeta(1)) \quad (4.9)$$

and

$$\zeta'(l) - ik_0 \zeta(l) = -2ik_0 e^{-ik_0 l} (c_4 + c_5 \zeta(0) + c_6 \zeta(l)), \quad (4.10)$$

the resulting integral equation is of a lot simpler form. Note that if  $A^+$  is set to 0 as it is for the subsequent numerical results, the coefficients  $c_1, \dots, c_6$  are given by

$$\begin{aligned} c_1 &= 1, & c_2 &= -\frac{iu'(0)}{4k_0 u(0)}, & c_3 &= 0, \\ c_4 &= 0, & c_5 &= 0, & c_6 &= \left( \frac{iu'(l)}{4k_0 u(l)} - \frac{(k_1 - k_0)}{2k_0} \right) e^{ik_0 l}. \end{aligned}$$

These coefficients follow very naturally from (4.5) and (4.6). Likewise, if we

were to set  $A^- = 0$  then the coefficients could be calculated in the same way but they would be different to the coefficients above.

If we regard the right-hand sides of (4.9) and (4.10) as known then they only contribute to the function  $\zeta_0$  and not to  $\hat{\zeta}$  in the decomposition  $\zeta = \zeta_0 + \hat{\zeta}$  referred to above. We find that the resulting integral equation has two forcing terms from the solution to  $\zeta_0$ , and the integral part comes from the solution to  $\hat{\zeta}$  which is purely in terms of a particular integral. Therefore, we have

$$\begin{aligned} \zeta(x) = & (c_1 + c_2\zeta(0) + c_3\zeta(l))e^{ik_0x} + (c_4 + c_5\zeta(0) + c_6\zeta(l))e^{-ik_0x} \\ & - \frac{i}{2k_0} \int_0^l e^{ik_0|x-t|} \rho(t)\zeta(t) dt. \end{aligned} \quad (4.11)$$

Although we have succeeded in rewriting our original boundary value problem as an integral equation, this equation is not ideal to work with as it is complex-valued. Hence we now need to transform this equation into a pair of real-valued integral equations. We do this by first noting that

$$e^{ik_0|x-t|} = \cos(k_0|x-t|) + i \sin(k_0|x-t|)$$

which is in turn equal to

$$\frac{e^{ik_0(x-t)} + e^{-ik_0(x-t)}}{2} + i \sin(k_0(x-t))$$

if we write the cosine function in terms of complex-valued exponentials. (Note that the modulus signs have been removed as the cosine function is an even function). This now allows us to rewrite (4.11) as

$$\begin{aligned} \zeta(x) = & (c_1 + c_2\zeta(0) + c_3\zeta(l) - I^-)e^{ik_0x} + (c_4 + c_5\zeta(0) + c_6\zeta(l) - I^+)e^{-ik_0x} \\ & - \frac{i}{2k_0} \int_0^l \sin(k_0|x-t|)\rho(t)\zeta(t)dt. \end{aligned} \quad (4.12)$$

where

$$I^\pm = \frac{i}{4k_0} \int_0^l e^{\pm ik_0t} \rho(t)\zeta(t)dt. \quad (4.13)$$

It now follows immediately that the solution to (4.11) can be written as a linear combination of the solution of the two real-valued integral equations by

$$\begin{aligned} \zeta(x) = & [c_1 + c_4 + (c_2 + c_5)\zeta(0) + (c_3 + c_6)\zeta(l) - I^- - I^+]\chi_1(x) \quad (4.14) \\ & + i[c_1 - c_4 + (c_2 - c_5)\zeta(0) + (c_3 - c_6)\zeta(l) - I^- + I^+]\chi_2(x) \end{aligned}$$

where

$$\chi_1(x) = \cos(k_0x) + \frac{1}{2k_0} \int_0^l \sin(k_0|x-t|)\rho(t)\chi_1(t)dt \quad (4.15)$$

and

$$\chi_2(x) = \sin(k_0x) + \frac{1}{2k_0} \int_0^l \sin(k_0|x-t|)\rho(t)\chi_2(t)dt. \quad (4.16)$$

These equations may be recast as equations on the real, infinite-dimensional Hilbert space  $X$  consisting of the real elements of  $L_2(0, l)$  by introducing two self-adjoint operators  $L$  and  $P$ , which map  $X$  into itself, according to

$$(L\chi)(x) = \frac{1}{2k_0} \int_0^l \sin(k_0|x-t|)\chi(t)dt$$

and

$$(P\chi)(x) = \rho(x)\chi(x).$$

If we also define  $f_1$  and  $f_2$  by  $f_1(x) = \cos(k_0x)$  and  $f_2(x) = \sin(k_0x)$  then  $\chi_1$  and  $\chi_2$  are solutions of the two operator equations

$$A\chi_1 = f_1 \quad (4.17)$$

and

$$A\chi_2 = f_2 \quad (4.18)$$

in  $X$  where  $A = I - LP$ . In order to determine the reflection and transmission coefficients, we need to find approximations to  $\chi_1$  and  $\chi_2$  and also to  $\zeta(0)$  and  $\zeta(l)$ .

# Chapter 5

## Methods of solution

As already stated, approximations to  $\chi_1$ ,  $\chi_2$ ,  $\zeta(0)$  and  $\zeta(l)$  are required. The functions  $\chi_1$  and  $\chi_2$  can be solved by numerous approximation methods for inhomogeneous integral equations whereas the approximations to  $\zeta(0)$  and  $\zeta(l)$  are not as straightforward. The following two results are useful in what follows.

Lemma: Suppose that  $I - LP$  is invertible and that  $\chi_1$  and  $\chi_2$  are the solutions of (4.15) and (4.16) where  $L$  and  $P$  are self-adjoint. Then  $(\chi_1, Pf_2) = (\chi_2, Pf_1)$ .

Proof:

$$\begin{aligned}(\chi_1, Pf_2) &= (P\chi_1, (I - LP)\chi_2) = ((I - LP)^*P\chi_1, \chi_2) = ((I - PL)P\chi_1, \chi_2) \\ &= (P(I - LP)\chi_1, \chi_2) = (Pf_1, \chi_2) = (\chi_2, Pf_1).\end{aligned}$$

in which  $*$  denotes the adjoint operator.

This lemma now leads us to the following result.

Result: With  $\zeta$ ,  $\chi_1$ ,  $\chi_2$ ,  $I^\pm$ ,  $L$  and  $P$  defined as before,  $\zeta(0)$  and  $\zeta(l)$  can be determined from the two simultaneous equations given by

$$\begin{aligned} 0 &= b_1 - (c_1 - b_4)iB_2 - (c_4 - b_1)iB_1 + (b_2 - (c_2 - b_5)iB_2 \\ &\quad - (c_5 - b_2)iB_1)\zeta(0) + (b_3 - (c_3 - b_6)iB_2 - (c_6 - b_3)iB_1)\zeta(l) \end{aligned}$$

$$\begin{aligned} 0 &= b_4 - (c_1 - b_4)iB_1 - (c_4 - b_1)i\bar{B}_2 + (b_5 - (c_2 - b_5)iB_1 \\ &\quad - (c_5 - b_2)i\bar{B}_2)\zeta(0) + (b_6 - (c_3 - b_6)iB_1 - (c_6 - b_3)i\bar{B}_2)\zeta(l), \end{aligned}$$

where

$$B_1 = \frac{1}{2}(A_{11} + A_{22}), \quad B_2 = \frac{1}{2}(A_{11} + 2iA_{12} - A_{22}),$$

$$A_{jk} = A_{kj} = \frac{1}{2k_0}(\chi_j, Pf_k), \quad j, k = 1, 2,$$

and

$$b_1 = \frac{1}{2}(c_1 + c_4), \quad b_2 = \frac{1}{2}(c_2 + c_5 - 1),$$

$$b_3 = \frac{1}{2}(c_3 + c_6), \quad b_4 = \frac{1}{2}(c_1 + c_4e^{-2ik_0l}),$$

$$b_5 = \frac{1}{2}(c_2 + c_5e^{-2ik_0l}), \quad b_6 = \frac{1}{2}(c_3 + c_6e^{-2ik_0l} - e^{-ik_0l}).$$

Also,

$$I^+ = b_1 + b_2\zeta(0) + b_3\zeta(l)$$

and

$$I^- = b_4 + b_5\zeta(0) + b_6\zeta(l).$$

These equations are not difficult to obtain. The expression for  $I^+$  arises from putting  $x = 0$  into (4.11) whereas putting  $x = l$  into (4.11) yields the expression for  $I^-$ . Substituting (4.14) into the plus option of (4.13) gives

$$I^+ = i(c_1 + c_2\zeta(0) + c_3\zeta(l) - I^-)B_2 + i(c_4 + c_5\zeta(0) + c_6\zeta(l) - I^+)B_1 \quad (5.1)$$

whereas putting (4.14) into the minus option of (4.13) gives

$$I^- = i(c_1 + c_2\zeta(0) + c_3\zeta(l) - I^-)B_1 + i(c_4 + c_5\zeta(0) + c_6\zeta(l) - I^+)\overline{B}_2 \quad (5.2)$$

The two simultaneous equations come from substituting the already known expressions for  $I^\pm$  into (5.1) and (5.2).

This last result tells us that a knowledge of the inner products  $A_{11}$ ,  $A_{12}$  and  $A_{22}$  will allow us to determine the values  $\zeta(0)$  and  $\zeta(l)$  via (4.17) and (4.18). This in turn will allow us to calculate the reflection and transmission coefficients. However, before we can solve for  $\zeta(0)$  and  $\zeta(l)$ , we need to determine approximations to  $\chi_1$  and  $\chi_2$ .

## 5.1 Inner product approximations

We attempt to find an approximation to the three inner products  $A_{jk}$ , ( $j, k = 1, 2$ ) by using variational calculus.

Consider the functional  $J_{jk} : X^2 \rightarrow \Re$  defined by

$$J_{jk}(p, q) = (f_j, q) + (p, Pf_k) - (Ap, q), \quad j, k = 1, 2.$$

If we let  $p = \chi_j + \delta\chi_j$  and  $q = \varphi_k + \delta\varphi_k$  where  $\delta\chi_j$  represents the variation in the approximation to  $\chi_j$  and  $\delta\varphi_k$  represents the variation in the approximation to  $\varphi_k$ , we obtain

$$\begin{aligned} J_{jk}(\chi_j + \delta\chi_j, \varphi_k + \delta\varphi_k) &= (f_j, \varphi_k + \delta\varphi_k) + (\chi_j + \delta\chi_j, Pf_k) \\ &\quad - (A(\chi_j + \delta\chi_j), \varphi_k + \delta\varphi_k) \end{aligned}$$

$$\begin{aligned}
&= J_{jk}(\chi_j, \varphi_k) + (f_j - A\chi_j, \delta\varphi_k) + (\delta\chi_j, Pf_k - A^*\varphi_k) \\
&+ O(\|\delta\chi_j\| \|\delta\varphi_k\|)
\end{aligned}$$

and hence we deduce that  $J_{jk}(p, q)$  is stationary when  $p = \chi_j$ ,  $q = \varphi_k$ , where  $A\chi_j = f_j$ ,  $j = 1, 2$ , and  $A^*\varphi_k = Pf_k$ ,  $k = 1, 2$ . The stationary value is

$$J_{jk}(\chi_j, \varphi_k) = (\chi_j, Pf_k) = 2k_0 A_{jk} \quad j, k = 1, 2,$$

and the approximation to the inner product is second-order accurate. Using this functional, approximations to  $A_{11}$ ,  $A_{12}$  and  $A_{22}$  can be found.

A simple and effective technique for evaluating the functional  $J_{jk}$  is the Rayleigh-Ritz method. This method involves approximating the solutions of  $\chi_1$  and  $\chi_2$  by choosing them to be members of some finite dimensional trial spaces.

We write

$$\chi_j \simeq \tilde{\chi}_j = \sum_{n=1}^N a_n^{(j)} \psi_n^{(j)}, \quad \varphi_k \simeq \tilde{\varphi}_k = \sum_{m=1}^N b_m^{(k)} \xi_m^{(k)}, \quad j, k = 1, 2,$$

where  $a_n^{(j)}$  and  $b_m^{(k)}$  are (real) coefficients to be determined and  $\psi_n^{(j)}$ ,  $\xi_m^{(k)}$  are trial functions.

Putting these expressions into the expression for  $J_{jk}$  yields

$$J_{jk}(\chi_j, \varphi_k) \simeq \sum_{m=1}^N b_m^{(k)}(f_j, \xi_m^{(k)}) + \sum_{n=1}^N a_n^{(j)}(\psi_n^{(j)}, Pf_k) - \sum_{m=1}^N \sum_{n=1}^N a_n^{(j)} b_m^{(k)}(A\psi_n^{(j)}, \xi_m^{(k)}).$$

To make this stationary within the trial space, we require

$$\frac{\partial J_{jk}}{\partial a_n^{(j)}} = \frac{\partial J_{jk}}{\partial b_m^{(k)}} = 0.$$

Enforcing these conditions leads us to following system.

$$(f_j, \xi_m^{(k)}) - \sum_{n=1}^N a_n^{(j)}(A\psi_n^{(j)}, \xi_m^{(k)}) = 0. \quad (5.3)$$

Choosing  $\xi_m^{(1)} = \psi_m^{(2)}$  and  $\xi_m^{(2)} = \psi_m^{(1)}$  is equivalent to solving (4.17) and (4.18) by the Petrov-Galerkin method. This is the method of choice in this dissertation. However, now we have determined a suitable method to solve the system and obtain approximations to the required inner products, we need to determine a good choice of test functions for  $\chi_1$  and  $\chi_2$ .

## 5.2 Choice of basis functions

As we wish to implement the Petrov-Galerkin method to derive approximations to the inner products  $A_{11}$ ,  $A_{12}$  and  $A_{22}$ , we need to choose good

finite-dimensional trial spaces from which the approximations are selected.

We seek an approximation to  $\chi$  which is the solution of the integral equation  $\chi = f + LP\chi$ . The Neumann series for this equation is given by

$$\chi = f + \sum_{n=1}^{\infty} (LP)^n f.$$

This series converges if  $\|LP\| < 1$  so we would expect that

$$\chi \simeq f + LPf + (LP)^2 f + \dots + (LP)^{N-1} f,$$

for some moderate value  $N$ . This structure is the motivation for choosing  $\chi$  to be an element of the  $N$ -dimensional trial space spanned by the individual terms of the Neumann series (it has also been shown by Porter and Stirling (1990) that this is a good choice of trial space). Hence we choose  $p$  of the form

$$p = \sum_{n=1}^N a_n (LP)^{N-1} f,$$

where the  $a_n$  are determined *via* the Petrov-Galerkin method.

# Chapter 6

## Numerical results

In this section, we attempt to reproduce various results that have already appeared in mathematical literature. In particular, an attempt has been made to reproduce Booij's results (1983), those of Chamberlain (1993), Porter and Staziker's (1995), and finally a ripple bed example initially done by Chamberlain and Porter (1995). In addition to these examples, some error analysis has been included and some examples are conducted using the modified-mild slope equation (MMSE) in order to draw a comparison with the mild slope equation (MSE).

### 6.1 Booij's test problem

Booij published a paper in 1983 discussing the accuracy of the MSE and presenting some numerical results comparing calculations using the MSE and the full linearised theory. In particular, he considered a ramp problem for

which he produced a graph of  $|R|$  against  $w_s$ , a dimensionless parameter. The paper presented by Chamberlain (1993) considered the reproduction of Booi's graph using a very similar method to the one set out in this dissertation. He produced results that to the naked eye seemed to be identical to the original set produced by Booi. To confirm the accuracy of our methods we are here again interested in reproducing Booi's results for the MSE.

In Booi's original paper, all length scaling is conducted with respect to the deep-water wavenumber  $\frac{\sigma^2}{g}$ . Chamberlain chose to non-dimensionalise all length values with respect to  $l$  and create a non-dimensional  $H(x)$  instead of the  $h(x)$  we have used here. In terms of our variables, the parameter  $w_s$  is

$$w_s = \frac{\sigma^2 l}{g}.$$

The scaled equilibrium depths on each side of the ramp were chosen to be 0.6 and 0.2 and the ramp itself was obviously linear. Accordingly, in our notation we have

$$h_0 = \frac{0.6g}{\sigma^2}, \quad h_1 = \frac{0.2g}{\sigma^2},$$

and our notation for the equation for the talud is

$$h(x) = h_0 \left(1 - \frac{2x}{3l}\right).$$

The choice of  $\frac{\sigma^2}{g}$  is arbitrary but account must be taken of the altered values for  $h_0$  and  $h_1$  as the equation for  $h(x)$  will change.

The program was run using  $\frac{\sigma^2}{g} = 1$  and for values of  $w_s$  between 0.05 and 6. The number of discrete points in each interval used for the numerical computation of the integrals was 200. This ensured that the step size was small which is crucial when performing numerical integration. For purposes of error determination, the exact solution to this problem was deemed to be a Petrov-Galerkin approximation with a twenty-dimensional trial space. By insisting that the error between this ‘exact’ solution and any lesser approximation be less than  $10^{-2}$ , it was found that a pair of trial spaces with dimension  $N = 2$  was required for  $w_s$  taking values between 0 and  $\simeq 0.7$ , but as  $w_s$  increased it was necessary to increase the trial space up to an ultimate dimension of  $N = 7$ . The reason for this is that as  $w_s$  increases,  $\|LP\|$  increases. This means that a larger trial space is required to keep the error under control. The graph produced is shown in figure(6.1) plotted on log-log axes (the axes used by Booij). The fully linear solution (courtesy of R. Porter) has been plotted as well.

To the naked eye, the MSE approximation appears to be identical to the approximation initially produced by Booij and then reproduced by Chamberlain. However there is some discrepancy between the full linear solution produced by Booij and the full linear solution produced here. Despite this fact though, we can conclude that the MSE has certainly detected the local maxima and minima in the graph in the correct places and has also provided an approximation that for the most part is fairly good.

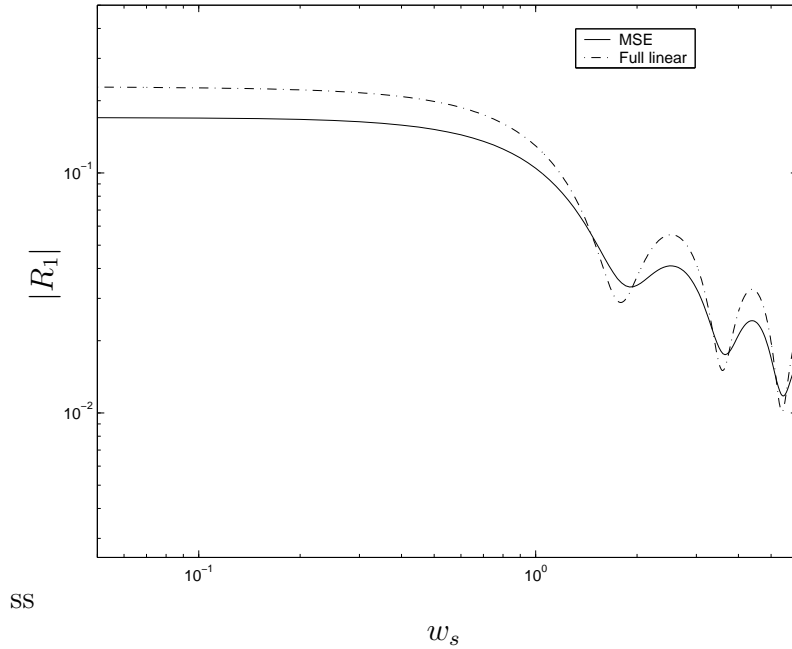


Figure 6.1: Reproduction of Booiij’s graph using our solution procedure plotted against the full linear solution.

### 6.1.1 Dimension of the trial spaces

As was stated at the start of the problem, the error between any approximation to  $|R_1|$  and the ‘exact’ solution was required to be no bigger than  $10^{-2}$ . However, the number of basis functions for  $\chi_1$  and  $\chi_2$  needed to achieve the desired level of accuracy will depend on the interval length  $l$ . Indeed, as the interval under consideration becomes larger, so will the dimension of the trial space needed to give the desired level of accuracy. This leads to an interesting question: how many terms are needed to produce a good level of accuracy? Obviously if a very large trial space comprising many terms were used, we would expect to get a very accurate answer. However, this may also be mathematically redundant as we may get the desired level of accuracy with a trial space consisting of relatively few terms. Figure (6.2) is a step

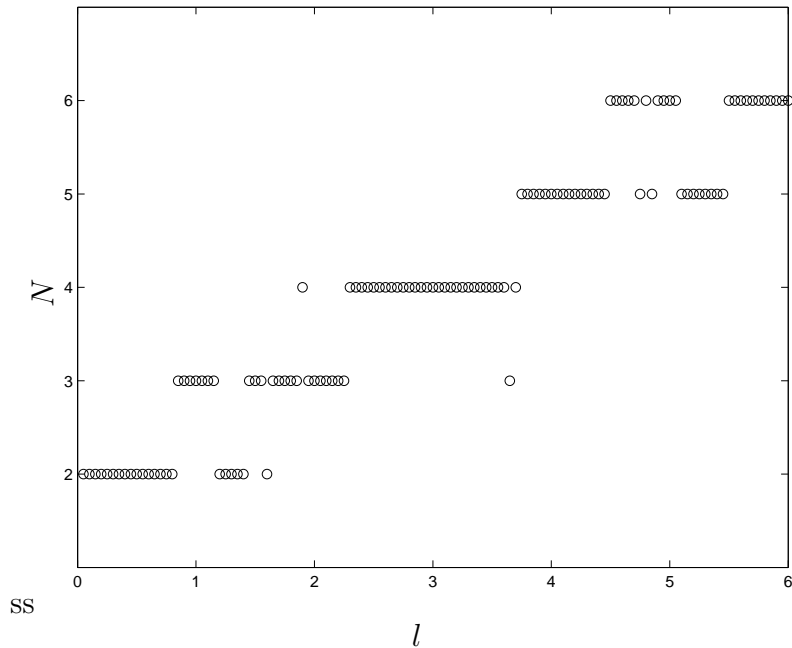


Figure 6.2: Number of basis functions needed to make the error  $< 10^{-2}$ .

graph that shows how many terms are required to produce the stated level of accuracy in the error. We have assumed that the ‘exact’ solution here is a Petrov-Galerkin approximation applied to a twenty-five dimensional trial space.

Figure (6.2) does not depict a smooth graph as the approximations to  $\chi_1$  and  $\chi_2$  can often become inaccurate for certain interval lengths but then become reasonably accurate again for other interval lengths. (In actuality however, once an approximation has become inaccurate it would not be used even if it recovers the desired level of accuracy for any other interval length). The reason approximations to  $\chi_1$  and  $\chi_2$  with small trial spaces become inaccurate as  $l$  increases is that the norms of the basis functions grow with  $l$ . Hence at  $l = 0.05$ , the basis functions become very small after the first two

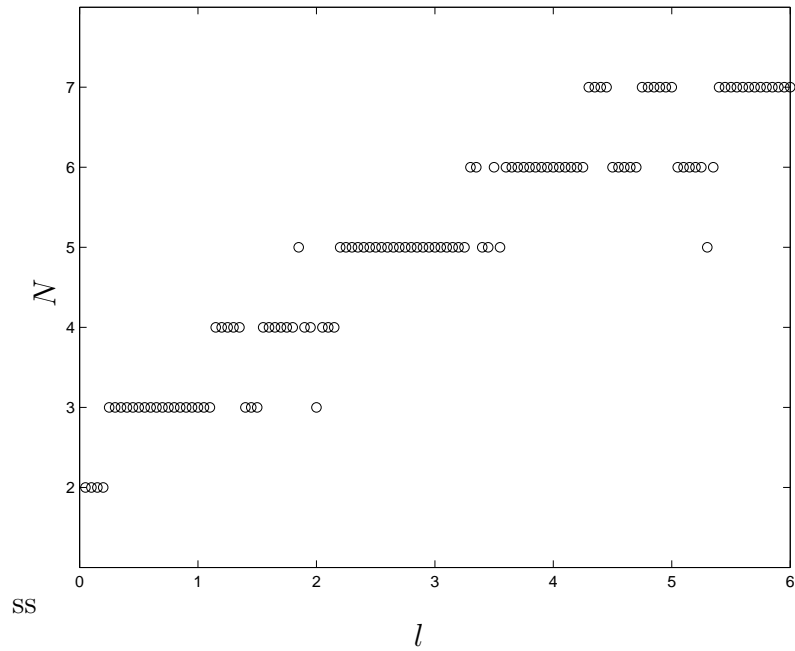


Figure 6.3: Number of basis functions needed to make the error  $< 10^{-4}$ .

terms, and indeed these first two terms added together would constitute a good approximation to the Neumann series. However at  $l = 6$ , the first two basis functions would no longer be much larger than the rest of the neglected terms. This means that a larger trial space must be selected to obtain an accurate answer. This step graph depicts this trend very well. Also it is worth noting that this trend would continue until the trial spaces needed for longer interval lengths would be very large.

Figure (6.3) depicts another step graph except that the error deemed acceptable is now  $< 10^{-4}$ . This graph as you would expect is very similar to the previous graph except that as the error tolerance is now smaller, more terms are needed to provide this error tolerance over every interval length.

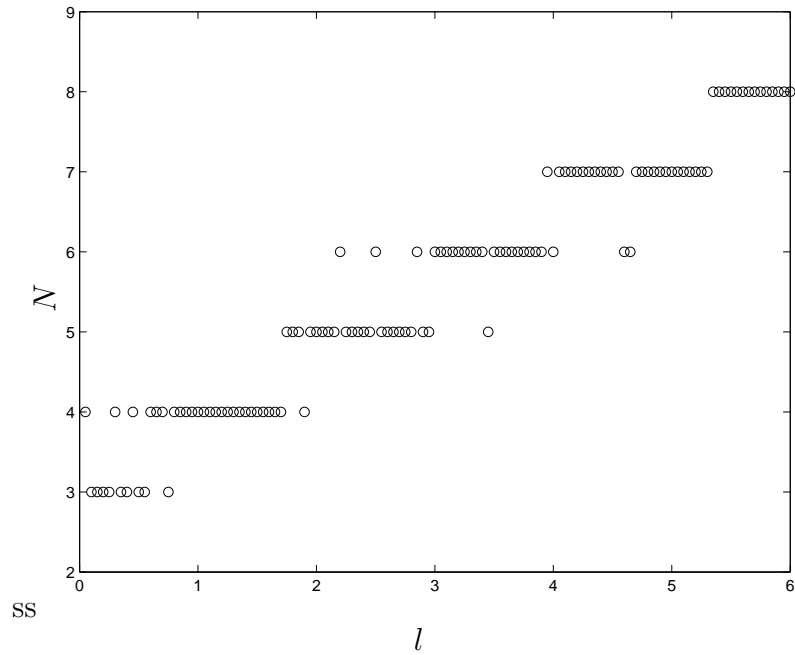


Figure 6.4: No. of basis functions needed to make the error  $< 10^{-6}$ .

Again, figure (6.4) depicts a similar trend as seen in figures (6.2) and (6.3).

If you attempt to specify the error between the ‘exact’ and approximate solutions to be no larger than  $10^{-7}$  then you would get a similar graph to the previous ones above but unfortunately the error cannot be specified to be  $< 10^{-8}$ . This is likely to be due to the disappointing accuracy of the trapezium rule and not the method as a whole as Chamberlain’s (1993) original integral equation method could recover answers correct to thirteen decimal places. Ideally, Gaussian integration would be used but that is a more difficult type of numerical integration to implement here as it would require integral smoothing when calculating the terms of the Neumann series. Hence, for computational simplicity, the use here of the composite trapezium rule.

### 6.1.2 Accuracy of the Neumann series

As mentioned earlier in this dissertation, the Neumann series for (4.17) and (4.18) would be expected to be equal to the unknown functions  $\chi_1$  and  $\chi_2$  if  $\|LP\| < 1$ . Unfortunately though it is impossible to calculate all the terms in the Neumann series due to the infinite summation. This means that we can only calculate a partial sum of the terms in the Neumann series and achieve an approximation. However most of the terms in the Neumann series will be very small and can be neglected. Hence we would still expect a partial sum of the first few terms of the Neumann series (say nine or ten for the most part) to produce a good approximation to  $\chi_1$  and  $\chi_2$ . As a result, if we were to omit the application of the Petrov-Galerkin method and use the partially summed Neumann series as our approximations to  $\chi_1$  and  $\chi_2$ , we would expect the reflection coefficient ( $|R_1|$ ) produced to be virtually identical to the Petrov-Galerkin approximation when the Neumann series converges, but very different when the Neumann series diverges. Figure (6.5) shows the graph produced of the Neumann series approximation plotted against the Petrov-Galerkin approximation when applied to Booij's test problem.

You can see from the graph that the reflection coefficients produced by both approximations coincide for  $l \lesssim 1.8$ . When we consider any larger intervals, the Neumann series diverges and produces a poor approximation to  $\|R_1\|$  whereas the Petrov-Galerkin continues to produce the correct values. We infer that for this problem,  $\|LP\| < 1$  for  $l \leq 1.8$ , and  $\|LP\| > 1$  for  $l \geq 1.8$ .

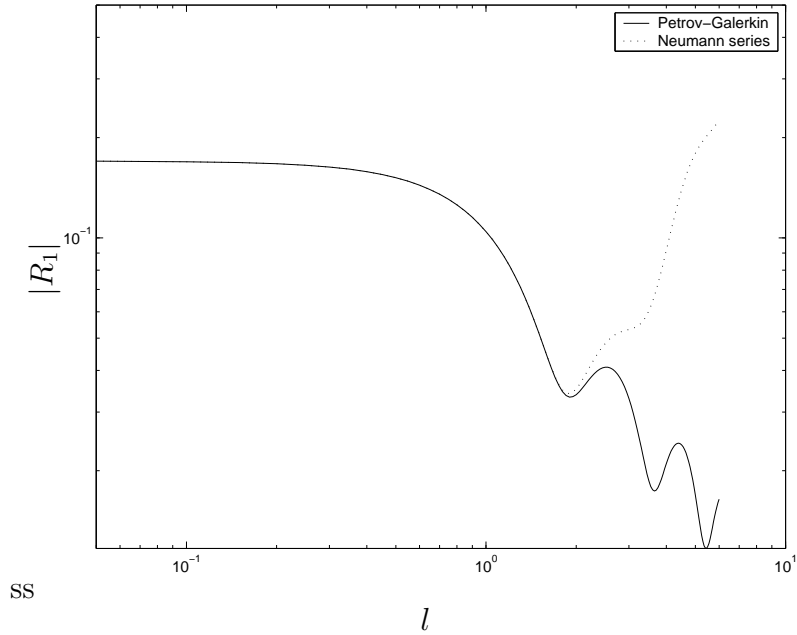


Figure 6.5: A comparison between the Petrov-Galerkin approximation and the Neumann series approximation applied to Booijs test problem.

### 6.1.3 Booijs test problem using the MSE and MMSE subject to two different sets of boundary conditions

In 1995, Porter and Staziker presented a paper that contained two graphs comparing the MSE and the MMSE applied to Booijs test problem (1983) subject to two different sets of boundary conditions. We now attempt to reproduce these graphs here.

It was mentioned in Chapter 4 that  $\phi'_0$  must be continuous at  $x = 0$  and  $x = l$  as otherwise equation (3.2) would not be satisfied. However, when we consider the modified mild-slope equation, the explicit appearance of  $h''$  implies that  $\phi'_0$  will, in general, be discontinuous at locations where  $h'$  is

discontinuous. If  $h'(x)$  is continuous then our current set of boundary conditions are correct, whereas if  $h'(x)$  is discontinuous at  $x = 0$  and/or  $x = l$ , then new boundary conditions are required.

Booij's test problem involves two slope discontinuities in  $h'$  at  $x = 0$  and  $x = l$ . This means that our existing boundary conditions are incorrect. The correct set of boundary conditions for this problem are

$$\zeta'(0) + ik_0\zeta(0) = 2ik_0 \left( 1 + \frac{iu_1(0)}{2k_0\sqrt{u(0)}} \right) - 2ik_0 \frac{iu'(0)}{4k_0u(0)}\zeta(0),$$

and

$$\begin{aligned} \zeta'(l) - ik_0\zeta(l) &= 2ik_0 \left( \frac{iu_1(l)}{2k_0\sqrt{u(0)}} h'(l) \right) \\ &- 2ik_0 \left( \frac{iu'(l)}{4k_0u(l)} - \frac{(k_1 - k_0)}{2k_0} \right) \zeta(l). \end{aligned}$$

The derivation of these boundary conditions can be seen in Porter and Staziker (1995).

Figure (6.6) shows the MSE and the MMSE applied to Booij's test problem with boundary conditions assuming  $\phi'_0$  is continuous at  $x = 0$  and  $x = l$ .

This graph seems to be identical to the graph of Porter and Staziker. In comparison to the fully linear solution, the approximations produced by the

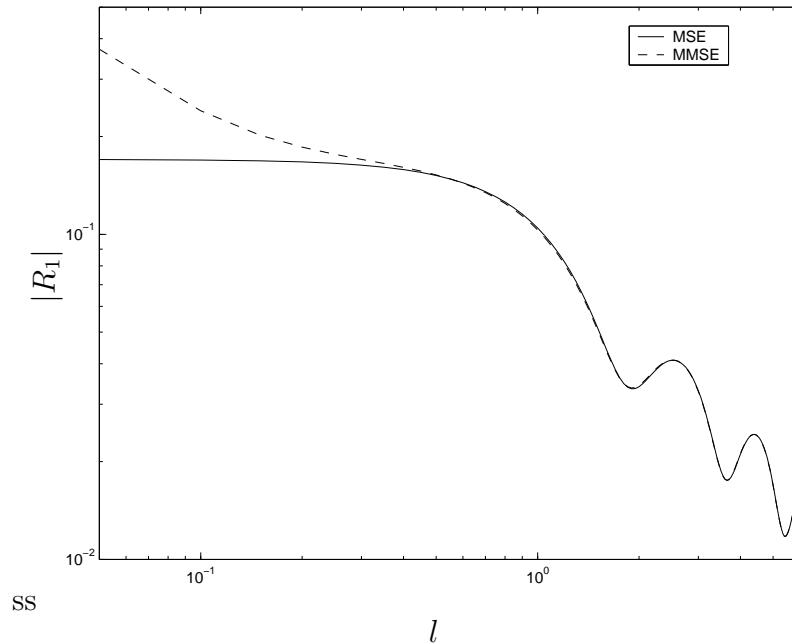


Figure 6.6: Comparison of the MSE and MMSE subject to continuous boundary conditions applied to Booiij's test problem.

MSE and the MMSE are not quite correct although they both do detect the correct trends of the coefficients. This is because the incorrect set of boundary conditions have been applied to the problem.

Figure (6.7) depicts both the MSE and the MMSE applied to Booiij's test problem subject to the boundary conditions assuming  $\phi'_0$  is discontinuous at  $x = 0$  and  $x = l$ . The solutions computed *via* both approximations this time is more accurate in comparison with the full linear solution plotted in figure (6.1). The approximation produced by the MSE is very different to the MMSE and the full linear solution when  $l$  is very small but eventually the solution converges to the same values as produced by the MMSE.

This graph is also identical to the naked eye to the graph produced by Porter

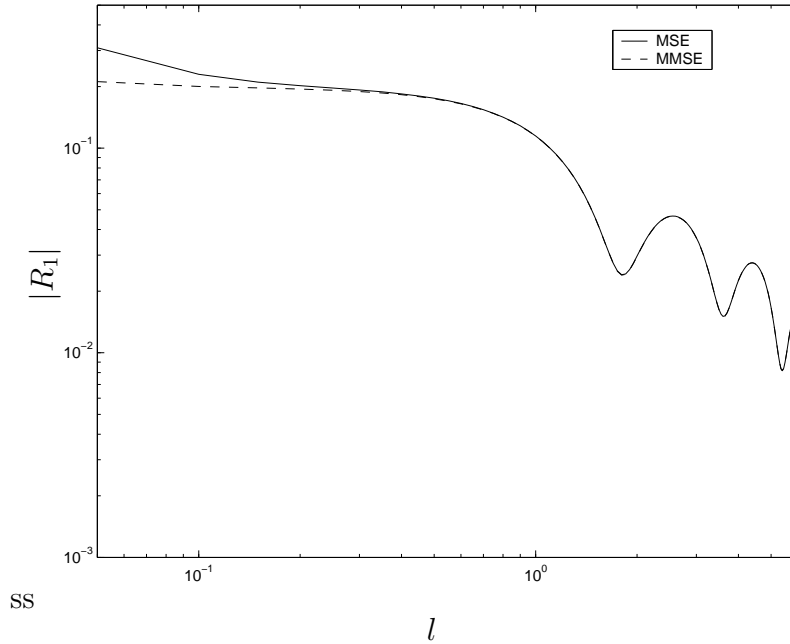


Figure 6.7: Comparison of the MSE and MMSE subject to discontinuous boundary conditions applied to Booijs’s test problem.

and Staziker.

## 6.2 The effects of different types of talud on the reflection coefficients

This example is again taken from the paper by Chamberlain (1993). In his paper, Chamberlain endeavoured to determine the effect of different types of talud on the reflection coefficient. He considered three different types of talud: a concave talud, a convex talud and a linear talud. The non-dimensional fluid depths to the left and right of each talud are 1 and 0.5 respectively. The equations for each talud are defined to be:

$$H_1(x) = \frac{1}{2} + \frac{1}{2}(x - 1)^2$$

for the convex talud,

$$H_2(x) = 1 - \frac{1}{2}x$$

for the linear talud, and

$$H_3(x) = 1 - \frac{x^2}{2}$$

for the concave talud. As discussed in the previous example, Chamberlain employed a non-dimensional scaling on his variables with respect to  $l$ . Thus his  $x$  above is defined to be equal to the  $x$  used in our notation divided through by  $l$ . Also, the above equations defining the shape of each talud need to be divided through by  $h_0$ . Therefore in our notation the shapes of the taluds become

$$h_1(x) = \frac{h_0}{2} \left( 1 + \frac{(x-l)^2}{l^2} \right),$$

$$h_2(x) = h_0 \left( 1 - \frac{x}{2l} \right),$$

$$h_3(x) = h_0 \left( 1 - \frac{x^2}{2l^2} \right),$$

where the subscripts 1, 2 and 3 correspond to the taluds of the same shape as in Chamberlain's example.

The final issue that needs consideration is the interval against which the  $|R_1|$  coefficients are plotted. Chamberlain originally plotted  $|R_1|$  against a parameter  $\omega$  which was defined to be equal to

$$\omega = \frac{l}{h_0},$$

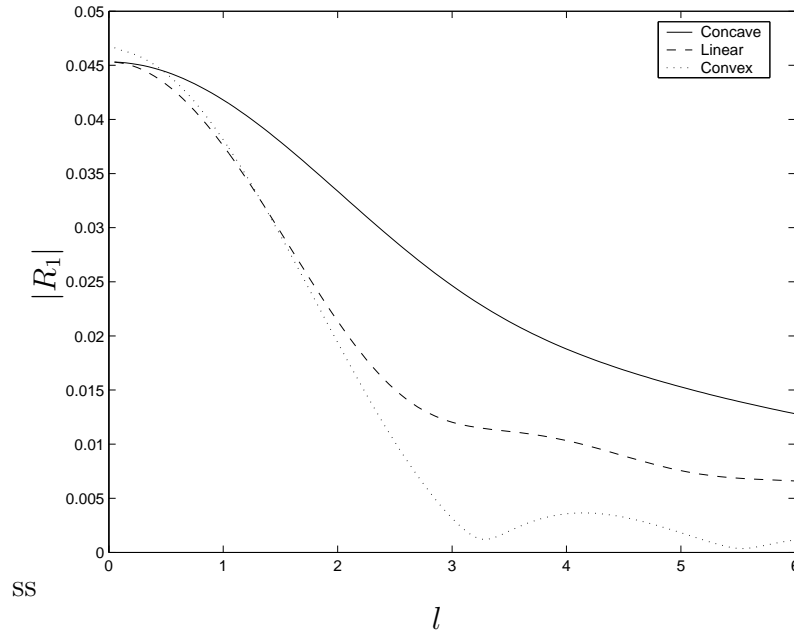


Figure 6.8: The effect of different bed shapes on  $|R_1|$ .

If we take  $h_0 = 1$  then the original parameter  $\omega$  is equivalent to  $l$ . Therefore we choose  $h_0 = 1$  and  $h_1 = 0.5$  to be consistent with the original problem.

Figure (6.8) shows the resulting graph.

This graph, like the Booij graph, is identical as far as the naked eye can tell to the graph produced by Chamberlain.

### 6.3 Wave scattering over ripple beds

It was mentioned at the start of the project that one reason why the MMSE was derived was due to the failure of the MSE to accurately predict wave scattering over ripple beds. In their paper on the derivation of the MMSE,

Chamberlain and Porter (1995) considered some examples of wave scattering over ripple beds to emphasise the difference in approximations produced by the MSE and the MMSE. They used some experimental data provided by Davies and Heathershaw (1984) and compared their solutions to these results in order to draw conclusions about accuracy. We now attempt to reproduce this here.

The function  $h(x)$  in this problem is now taken to be

$$h(x) = h_0 - d \sin\left(\frac{2n\pi x}{l}\right), \quad 0 < x < l$$

where  $n$  is the number of ripples. The real constant  $d$  will be defined shortly. This bedform therefore consists of a sequence of  $n$  sinusoidal ripples about the mean depth  $z = -h_0$ .

The examples considered by Chamberlain and Porter (1995) involved the non-dimensionalisation of the parameters in the problem. They plotted a graph of  $|R_1|$  against a parameter  $\beta$  in the interval  $(0.5, 2.5)$ , which is defined in our notation as

$$\beta = \frac{lk_0}{n\pi}.$$

If we introduce the real constant  $\delta$  defined by

$$\delta = \frac{d}{h_0},$$

and fix a particular  $\beta \in (0.5, 2.5)$  we obtain

$$k_0 h_0 = \frac{\beta \pi}{20 \delta},$$

$$l = n \pi \beta \tanh(k_0 h_0),$$

$$h_0 = k_0 h_0 \tanh(k_0 h_0),$$

so provided that  $\delta$  and  $n$  are specified at the start of every problem, we can calculate every necessary quantity.

Figure (6.9) shows the approximations produced by the MSE and the MMSE to a ripple bed problem with  $n = 4$  and  $\delta = 0.32$ .

This was the first example considered by Chamberlain and Porter when applying the MMSE and the MSE to a ripple bed problem. This graph appears to be identical to the graph that they produced. The graph itself shows a good agreement in the approximations produced by both equations. Both the MSE and the MMSE pick up the first order resonance peak near  $\beta = 1$ .

Figure (6.10) depicts a similar example except that now the  $n = 10$  and  $\delta = 0.16$ . This time the approximations produced by both equations are

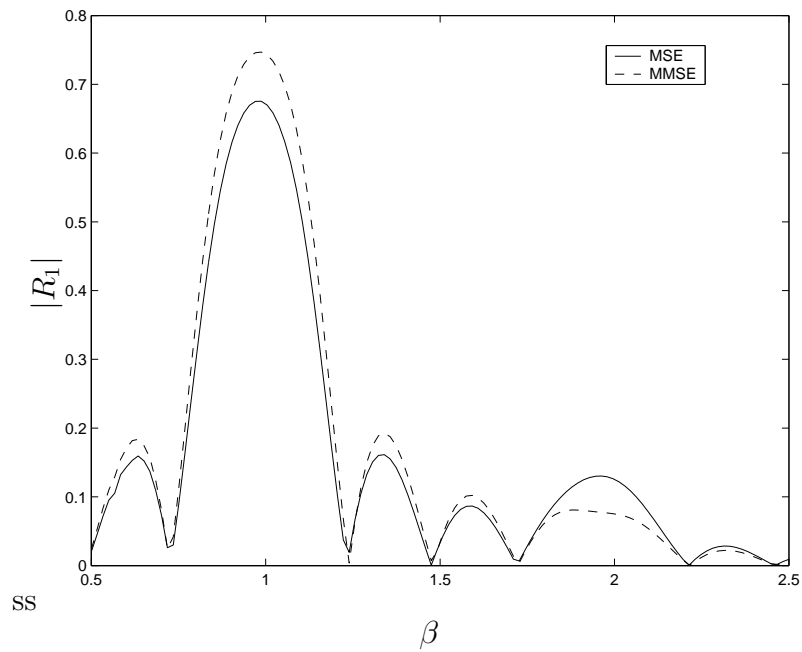


Figure 6.9: Comparison of computed reflection coefficients for a ripple bed problem with  $n = 4$  and  $\delta = 0.32$ .

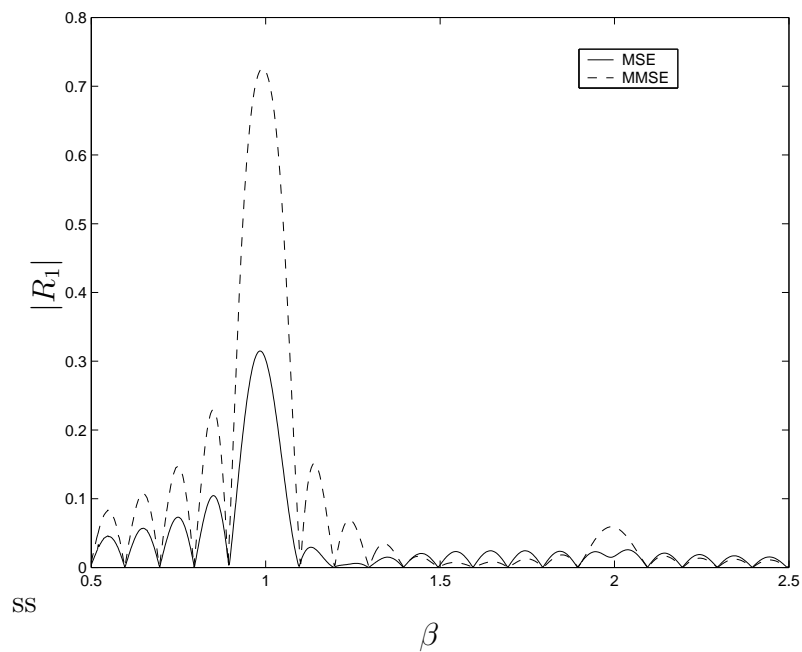


Figure 6.10: Comparison of computed reflection coefficients for a ripple bed problem with  $n = 10$  and  $\delta = 0.16$ .

very different. The MSE picks out that there should be a peak at  $\beta = 1$  but it does not predict the correct value at the peak. It also completely misses the peak at  $\beta = 2$ . The MMSE does however pick out the correct values at the peak at  $\beta = 1$  and  $\beta = 2$ . This graph is again identical to the naked eye to the graph produced by Chamberlain and Porter.

# Chapter 7

## Conclusions

The scattering of small-amplitude waves by variations in a one-dimensional topography has been examined. Rather than attempting to solve the original boundary value problem that was formulated as an ordinary differential equation, the problem has been converted to a complex-valued integral equation and then split up into two further real-valued integral equations. This method is very similar to the method used by Chamberlain (1993) except that the integral equation formed is not self-adjoint and the function  $\rho$  is not forced to be entirely one-signed. This method does not have the advantage of providing an integral equation for which we can easily derive error bounds for but the implementation of the approximation is made considerably more simple.

We have seen that this method has proved just as effective as the original integral equation method used by Chamberlain, and that it can easily reproduce the results that other people have obtained using numerically solving differential equation techniques. In addition, some calculations have been

performed using the modified mild-slope equation which has never been done before using integral equation techniques. Finally, the conclusion that the mild slope approximation is not as accurate an approximation as the modified mild slope approximation has been drawn.

# Bibliography

- [1] BERKHOFF, J. C. W. 1973 Computation of combined refraction-diffraction. *Proc.13th Int. Conf. on Coastal Eng*, 471–490
- [2] BERKHOFF, J. C. W. 1976 Mathematical models for simple harmonic linear water waves. *Report W 154-IV – Delft Hydr*
- [3] BOOIJ, N. 1983 A note on the accuracy of the Mild-Slope equation. *Coastal Engineering* **7**, 191–205
- [4] CHAMBERLAIN, P. G 1993 Wave scattering over uneven depth using the mild slope equation. *Wave Motion* **17**, 267–285.
- [5] CHAMBERLAIN, P. G. & PORTER, D. 1995 The modified mild-slope equation. *J. Fluid Mech.* **291**, 393–407.
- [6] DAVIES, A. G. & HEATHERSHAW, A. D. 1984 Surface-wave propagation over sinusoidally varying topography. *J. Fluid Mech.* **144**, 419–443
- [7] PORTER, R. 2005 Private communication.
- [8] PORTER, D. & STAZIKER, D. J. 1995 Extensions of the mild-slope equation. *J. Fluid Mech.* **300**, 367–382.

- [9] PORTER, D. & STIRLING, D. S. G. 1990 Integral Equations. *Cambridge University Press, Cambridge*